PCCP

ROYAL SOCIETY OF CHEMISTRY

COMMUNICATION

View Article Online
View Journal | View Issue

Cite this: *Phys. Chem. Chem. Phys.*, 2024, **26**, 19083

Received 11th June 2024,
Accepted 30th June 2024

DOI: 10.1039/d4cp02363c

rsc.li/pccp

Optical trapping of nanoclusters formed in a temperature-responsive ionic liquid aqueous solution under focused near-infrared laser irradiation†

Maho Tanaka, Rai Kobayashi, Yasuyuki Tsuboi and Ken-ichi Yuyama *

Confining molecules and ions at a specific position in a solution enables the control of chemical reactions and analysis of tiny amounts of substances. Here, we demonstrate local condensation of a temperature responsive ionic liquid using optical tweezers. Two kinds of microdroplets are prepared through phase separation or nanocluster formation under irradiation of a near-infrared laser beam. The droplet formation mechanism is discussed in view of the evolution of an optical potential well and the local temperature distribution.

The concentration of molecules and ions is a critical parameter in various chemical processes in solution. Utilization of optical forces is one of the potential approaches to tune concentrations in a spatially and temporally controlled manner. A focused laser beam is known to generate an optical force.[1] Its magnitude is determined by the polarizability (α_{pol}) of the target object and the gradient of light intensity.[2] If the polarizability is larger than that of the surrounding medium (solvent molecules), the gradient acts as an attractive force toward the focal spot. Therefore, the laser generates an optical potential well, U_{opt}:

$$U_{opt} = -\frac{1}{2}\alpha_{pol}E^2 \quad (1)$$

where E is the electric field vector of the incident light. If U_{opt} is energetically deep compared to the thermal energy (kT), the object is stably trapped. This technique is known as optical tweezers and provides us with a powerful tool to trap and manipulate colloidal particles on the nano- and micro-scale in solution.[3–8] The polarizability (α_{pol}) is proportional to the volume of the object, so U_{opt} becomes shallow for small volumes of the material. This is a major reason why it is difficult to optically trap molecules and molecular ions with single beam optical tweezers.

One of the interesting systems to apply optical tweezers is within solutions that exhibit lower critical solution temperature (LCST)-type phase separation behavior.[9,10] Aqueous solutions of some polymers,[11–14] alcohols,[15] and ionic liquids (ILs)[16,17] exhibit such phase separation behavior. In these solutions, single droplet formation can be induced under irradiation of a focused near-infrared laser beam. The droplet formation is triggered by laser heating through the absorption of incident photons due to the overtone of OH vibrational modes within the solvent water molecules. When the local temperature reaches a critical point, condensates are formed through phase separation. These are attracted together by the strong optical force due to their larger size. The gathered condensates merge with one other, forming a single liquid droplet that can grow up to approximately 10 μm in diameter.

In the present study, we show the temperature dependence of the laser-induced single droplet formation in an IL/water mixture that exhibits LCST-type phase separation behavior. Even when the local temperature is below the critical point, a single droplet is formed due to the formation and subsequent trapping of nanoclusters. Notably, the droplet is composed of highly concentrated ILs. The current approach provides a new opportunity to concentrate molecules and molecular ions at specific positions.

The IL used is tetrabutylphosphonium 2,4-dimethylbenzenesulfonate ($[P_{4444}]^+[2,4\text{-}MeSo_3]^-$) (Fig. 1a). For optical tweezers experiments, we prepared an IL/water mixture which has an IL mass fraction of 0.094 and this leads to a critical temperature of 49 °C.[18] Fig. 1b shows the size distribution in the IL solution, which was obtained by DLS (dynamic light scattering) measurements at different solution temperatures. At 25 °C, the solutes are distributed at a size of less than 5 nm, indicating that the IL exists as individual cations and anions. Upon heating the solution to 55 °C, micrometer-sized IL-rich droplets were obtained. This is the result of phase separation. It should be noted that the IL evolved into nanoclusters with a diameter of about 10 nm at 45 °C, which is below the critical temperature.

Department of Chemistry, Graduate School of Science, Osaka Metropolitan University, 3-3-138 Sugimoto Sumiyoshi-ku, Osaka-shi, 558-8585, Japan. E-mail: k-yuyama@omu.ac.jp

† Electronic supplementary information (ESI) available. See DOI: https://doi.org/10.1039/d4cp02363c

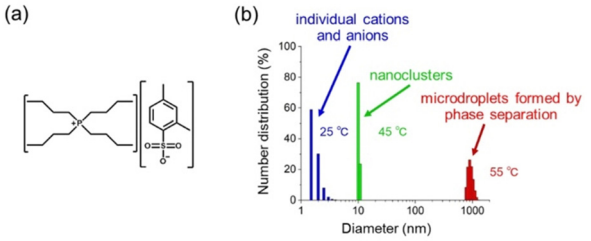

Fig. 1 (a) Molecular structure of tetrabutylphosphonium 2,4-dimethylbenzenesulfonate ($[P_{4444}]^+[2,4\text{-}MeSo_3]^-$). (b) Size distribution of $[P_{4444}]^+[2,4\text{-}MeSo_3]^-$ in the aqueous solution with an IL mass fraction of 0.094 at different temperatures.

It has been previously reported that nanoclusters are formed in a 50 wt% aqueous solution of the same IL ($[P_{4444}]^+[2,4\text{-}MeSo_3]^-$).[19] A similar size increase was also reported for a water/$[P_{4444}]^+[CF_3COO]^-$ mixture as the temperature was increased leading up to the critical point.[20] In their report, the aggregation behavior was supported not only by DLS measurements but also by additional experimental techniques, like cryo-transmission electron microscopy, suggesting that the nanoclusters have a micellar-like structure. However, their detailed structure is still unclear. At the present stage, the nanoclusters are considered fuzzy aggregates composed of ILs and water molecules. Despite the lack of details, they surely have a detectable lifetime and a size larger than individual anions and cations. The formation of nanoclusters deepens U_{opt} due to their larger size, leading to efficient optical trapping and assembling.

Single droplet formation can be observed during optical transmission imaging under irradiation of a 1064 nm-laser beam at different solution temperatures. Fig. 2 shows the time evolution of optical micrographs in the solution at 36 and 25 °C. The power of the laser after passing through the objective lens (×100, numerical aperture; 1.45) was tuned to 630 mW. The solution was initially homogeneous, and nothing was seen under the microscope. Due to the optical tweezing effect, at 36 °C, a small liquid droplet formed at the focal spot, and increased in volume while remaining stably trapped (Fig. 2a). The diameter of the droplet reached 8.5 μm at 420 s. The focal spot size was approximately 1.0 μm, which is determined by the wavelength of the incident laser and numerical aperture of the objective lens. Thus, the droplet diameter was much larger compared to the focal spot size. Compared to the heated conditions (Fig. 2a), a small droplet formed in the solution at room temperature (25 °C) (Fig. 2b). The diameter of the droplet was 1.9 μm at 600 s. This size was close to that of the focal spot.

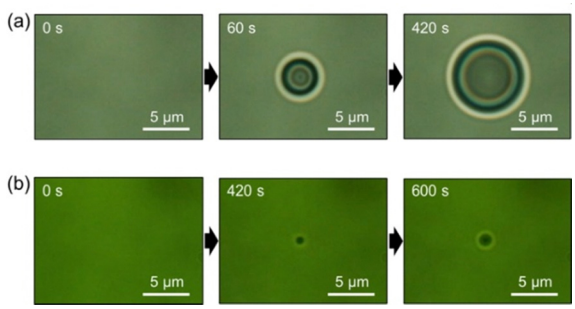

Fig. 2 Optical transmission micrographs around the laser focus on the solutions heated at (a) 36 and (b) 25 °C.

The difference in the droplet size is attributed to the different distribution of solution temperature. The incident 1064 nm-laser light is absorbed by solvent molecules, and the solution temperature is elevated around the laser focus. It has been reported that the local temperature rise in optical tweezing can be calculated as a function of the absorption coefficient (α_{abs}), the thermal conductivity (k), and the input laser power (P).[21] The elevation (ΔT) is calculated using the following equation:

$$\Delta T = 0.75\frac{\alpha_{abs}}{k}P. \quad (2)$$

The IL mole fraction of the initial solution is approximately 4.0×10^{-3}. Due to the low IL concentration, we assumed the initial solution to be just neat water and calculated the local temperature elevation using parameters of water (14.5 m^{-1} for α_{abs}, 0.59 W m^{-1} K^{-1} for k and 0.63 W for P). The elevation was estimated at 12 K. The solution temperature was tuned at 36 and 25 °C, so that the local temperature is expected to be 48 and 37 °C under respective conditions.

In the former case, the local temperature is close to the critical point, and phase separation should occur around the laser focus. The IL plays a role in enhancing the temperature rise because its thermal conductivity is lower than that of water.[16] Once a droplet is formed at the focal spot, the temperature distribution becomes both higher and wider. Further phase separation proceeds outside the droplet, leading to its growth. Hereafter, we call this large droplet a "phase separation droplet." For the solution temperature at 25 °C, laser heating similarly occurs, but the local temperature is below the critical point. Thus, nanoclusters are formed without phase separation. They are gathered in U_{opt}, evolving to a single droplet. We name this droplet a "nanocluster droplet" herein.

A fluorescence probe was used for characterization of these two droplets. We added a solvatochromic fluorescent dye (coumarin 153) of 1.3 μM to the initial solution. The probe molecules were extracted to a droplet through hydrophobic interactions and examined by fluorescence imaging and microspectroscopy. Coumarin 153 exhibits different emission colors depending on the local environment because the peak position of an intramolecular charge transfer band is sensitive to the polarity of the surrounding medium.[22] With an increase in the IL concentration, the polarity of the solution is decreased, and the emission maximum shifts to a short wavelength (Fig. 3a and b).

We also measured fluorescence decay curves at different IL concentrations (Fig. 3c). The average lifetimes were 3.0, 3.8, and 4.9 ns for the solutions with IL mass fractions of 0.1, 0.7, and 0.9, respectively. The fluorescence lifetime increases with the IL concentration (Fig. 3d). It is reported that the fluorescence decay time of coumarin 153 fluctuates depending on solvents

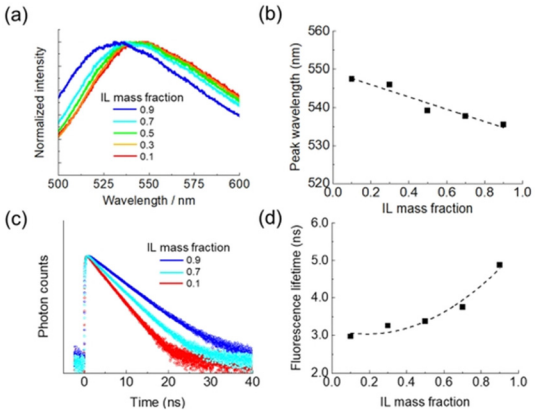

Fig. 3 (a) Fluorescence spectra of coumarin 153 in the IL solutions with different concentrations. (b) Plot of emission peaks against the IL mass fraction. The dotted line is a fitting curve. (c) Fluorescence decay curves of coumarin 153 in the IL solutions with different concentrations. (d) Plot of the fluorescence lifetime against the IL mass fraction. The dotted line is a fitting curve. The concentration of coumarin 153 is 1.3 μM in all solutions.

but exhibits no correlation with their polarity.[23] We consider that viscosity is a critical factor in the results of Fig. 3c and d. In general, ILs have viscosities 100–1000 times higher than those of traditional molecular solvents.[24] The viscosity of an IL/water mixture increases along with the IL concentration. Consequently, the vibrational or rotational motion of the probe molecule is suppressed, and the contribution of non-radiative relaxation becomes small, elongating the fluorescence lifetime.

Fig. 4a and b show fluorescence images of a phase separation droplet and a nanocluster droplet, respectively. The former showed yellow fluorescence, while the latter was green emissive. This difference in the emission color indicates that the IL concentration of a nanocluster droplet is higher than that of a phase separation droplet. Emission spectra of respective droplets are presented in Fig. 4c. The emission peaks were observed at 541.7 nm for a phase separation droplet and 534.7 nm for a nanocluster droplet. Based on the calibration curve of Fig. 3b, the IL mass fraction of the phase separation droplet was estimated to be 0.47. In our previous paper, the concentration was also measured by Raman microspectroscopy, and a similar value was obtained.[16] The nanocluster droplet was calculated to have an IL mass fraction of 0.90. This concentration is much higher compared to a phase separation droplet. A nanocluster droplet exhibits very slow dissolution after switching off the laser. It remains stable for more than 30 minutes without laser irradiation, indicating the high IL concentration.

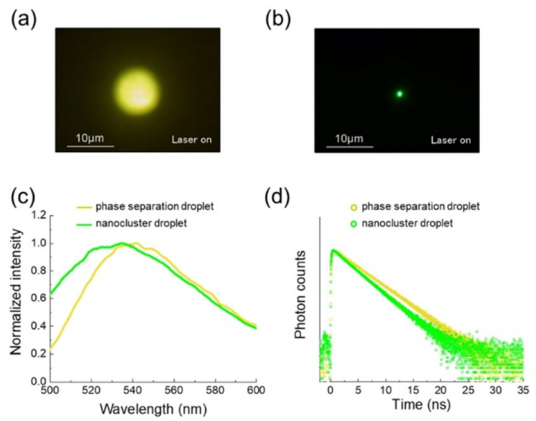

Fig. 4 (a) Fluorescence images of (a) a phase separation droplet and (b) a nanocluster droplet. (c) Fluorescence spectra and (d) decay curves of respective droplets.

We also measured the fluorescence lifetime of the droplets (Fig. 4d). The decay curves were collected for the whole wavelength of the emission. The fluorescence lifetime was 3.6 ns for a phase separation droplet. A nanocluster droplet exhibited a lifetime of 3.0 ns, which was shorter than that of a phase separation droplet. The IL concentration in a nanocluster droplet is high compared to a phase separation droplet, so that the result of Fig. 4d is inconsistent with the trend of Fig. 3d. We infer that this result is ascribed to the dye concentration in the droplet.

It is reported that coumarin 153 in EtOH solution exhibits a fluorescence decay curve composed of multi components.[25] The monomeric dye present in the solution shows a fluorescence lifetime of 4.8 ns. The dye forms H-aggregates with the concentration increase. Their fluorescence lifetime is shorter than that of the monomeric form. As the size of the aggregates increases, the fluorescence blue shifts, and the lifetime becomes shorter. We consider that, in the current experiment, coumarin 153 molecules are efficiently extracted to a nanocluster droplet with high IL concentration and high hydrophobicity. They are highly concentrated in the droplet, possibly existing as aggregates rather than in monomeric form. As a result, the blue-shifted fluorescence with a reduced lifetime is observed in a nanocluster droplet.

The nanocluster formation and subsequent trapping is likely induced even inside a phase separation droplet. In our previous paper, we showed the dissolution behavior of a phase separation droplet after switching off the laser.[16] The droplet decreased in its size, and only a small droplet with a diameter of 1.0 μm remained in the solution. The remaining small droplet exhibited green emission of coumarin 153, and its IL mass fraction was estimated to be 1.0. Thus, a phase separation droplet has a core–shell structure. Since a core and a nanocluster droplet have similar IL concentrations and sizes, we consider that the core is formed by the formation and trapping of nanoclusters at the laser focus inside a phase separation droplet.

Fig. 5 shows a schematic illustration of the possible dynamics of the droplet formation. Using optical tweezers at 36 °C, the solution temperature reaches the critical point, and phase separation is locally induced to form a small droplet. Subsequently, the temperature elevates, and its distribution widens because of the low thermal conductivity of the IL. Further phase separation occurs outside the laser focus due to the widened temperature distribution, leading to growth of the droplet. Thus, the size of a phase separation droplet is determined by the temperature distribution (Fig. 5a). For

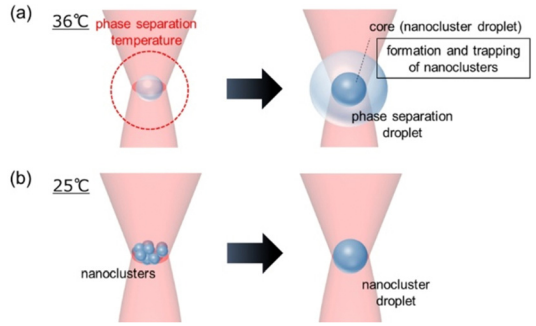

Fig. 5 A schematic illustration of the possible formation dynamics of (a) a phase separation droplet and (b) a nanocluster droplet.

optical tweezers at 25 °C, temperature at the laser focus is below the critical point. Nanoclusters are formed in a photo-thermal process without phase separation. They are confined in U_{opt} and evolve to a single droplet with a size similar to the focal volume (Fig. 5b). It is likely that a nanocluster droplet is also prepared at the focal spot inside a phase separation droplet, forming a core–shell structure (Fig. 5a).

Here, we discuss the concentration of the droplets. A phase separation droplet grows outside the laser focus, so that its IL concentration is determined to make the droplet thermodynamically stable at the given temperature. On the other hand, a nanocluster droplet is confined in U_{opt}. Its concentration and size are tuned to make the droplet optically stable. The polarizability in eqn (1) is a function of the refractive index of a target object and its volume. These two parameters should be increased in the trapping process to deepen U_{opt}. Thus, the gathered nanoclusters composed of ILs and water molecules are merged with each other to have a larger size. In addition, the IL concentration is also increased to have the higher refractive index because generally ILs have high refractive indices compared to water.[26] As a result, a single droplet with a highly concentrated IL is confined in the focal volume where U_{opt} is formed.

In conclusion, we have demonstrated single droplet formation by optical tweezers in a thermo-responsive IL aqueous solution at different temperatures. A thermodynamically stable droplet is formed through local phase separation under heating conditions. On the other hand, an optically stable dense droplet is prepared at room temperature. The current approach provides a new opportunity to tune the concentration of molecular ions in a spatially and temporally controlled manner. Notably, the latter droplet can efficiently extract and highly condense dye molecules due to high IL concentrations, possibly applicable to microanalysis of a tiny amount of molecules.

This work was financially supported by JSPS KAKENHI (grant numbers JP20H02550 JP20K05242 JP23H04600) and by JST, CREST (grant number JPMJCR1903). Also, the authors are grateful for financial support from the CANON Foundation.

Data availability

Data sharing is not applicable to this article as no datasets were generated or analysed during the current study.

Conflicts of interest

There are no conflicts to declare.

Notes and references

1 A. Ashkin, J. M. Dziedzic, J. E. Bjorkholm and S. Chu, Observation of a single-beam gradient force optical trap for dielectric particles, *Opt. Lett.*, 1986, **11**, 288–290.
2 Y. Harada and T. Asakura, Radiation forces on a dielectric sphere in the Rayleigh scattering regime, *Opt. Commun.*, 1996, **124**, 529–541.
3 A. Ashkin, Optical trapping and manipulation of neutral particles using lasers, *Proc. Natl. Acad. Sci. U. S. A.*, 1997, **94**, 4853–4860.
4 D. G. Grier, A revolution in optical manipulation, *Nature*, 2003, **424**, 810–816.
5 L. Jauffred, A. C. Richardson and L. B. Oddershede, Three-Dimensional Optical Control of Individual Quantum Dots, *Nano Lett.*, 2008, **8**, 3376–3380.
6 A. S. Urban, A. A. Lutich, F. D. Stefani and J. Feldmann, Laser Printing Single Gold Nanoparticles, *Nano Lett.*, 2010, **10**, 4794–4798.
7 S. E. S. Spesyvtseva and K. Dholakia, Trapping in a Material World, *ACS Photonics*, 2016, **3**, 719–736.
8 R. Bresolí-Obach, T. Kudo, B. Louis, Y.-C. Chang, I. G. Scheblykin, H. Masuhara and J. Hofkens, Resonantly Enhanced Optical Trapping of Single Dye-Doped Particles at an Interface, *ACS Photonics*, 2021, **8**, 1832–1839.
9 S.-A. Mukai, N. Magome, H. Kitahata and K. Yoshikawa, Liquid/liquid dynamic phase separation induced by a focused laser, *Appl. Phys. Lett.*, 2003, **83**, 2557–2559.
10 S. Mukai, H. Kitahata and K. Yoshikawa, Dynamical phase separation under laser scanning, *Chem. Phys. Lett.*, 2005, **402**, 529–534.
11 J. Hofkens, J. Hotta, K. Sasaki, H. Masuhara, T. Taniguchi and T. Miyashita, Molecular Association by the Radiation Pressure of a Focused Laser Beam: Fluorescence Characterization of Pyrene-Labeled PNIPAM, *J. Am. Chem. Soc.*, 1997, **119**, 2741–2742.
12 J. Hofkens, J. Hotta, K. Sasaki, H. Masuhara and K. Iwai, Molecular Assembling by the Radiation Pressure of a Focused Laser Beam: Poly(N-isopropylacrylamide) in Aqueous Solution, *Langmuir*, 1997, **13**, 414–419.
13 M. Matsumoto, T.-A. Asoh, T. Shoji and Y. Tsuboi, Formation of Single Double-Layered Coacervate of Poly(*N*,*N*-diethylacrylamide) in Water by a Laser Tweezer, *Langmuir*, 2021, **37**, 2874–2883.
14 T. Nagai, L. Jie, S. Teranishi, K. Yuyama, T. Shoji, Y. Matsumura and Y. Tsuboi, Förster Resonance Energy Transfer Control by Means of an Optical Force, *Adv. Opt. Mater.*, 2024, 2400302.
15 N. Kitamura, K. Konno and S. Ishizaka, Laser-Induced Single Microdroplet Formation and Simultaneous Water-to-Single Microdroplet Extraction/Detection in Aqueous 1-Butanol Solutions, *Bull. Chem. Soc. Jpn.*, 2017, **90**, 404–410.

16 M. Tanaka, Y. Tsuboi and K. Yuyama, Formation of a core–shell droplet in a thermo-responsive ionic liquid/water mixture by using optical tweezers, *Chem. Commun.*, 2022, **58**, 11787–11790.
17 M. Tanaka, I. Kuramichi, Y. Tsuboi and K. Yuyama, Confinement and aggregation of colloidal particles in an ionic liquid microdroplet formed by optical tweezers, *Jpn. J. Appl. Phys.*, 2022, **61**, 100901.
18 Y. Kohno, H. Arai, S. Saita and H. Ohno, Material design of ionic liquids to show temperature-sensitive LCST-type phase transition after mixing with water, *Aust. J. Chem.*, 2011, **64**, 1560–1567.
19 H. Kang, D. E. Suich, J. F. Davies, A. D. Wilson, J. J. Urban and R. Kostecki, Molecular insight into the lower critical solution temperature transition of aqueous alkyl phosphonium benzene sulfonates, *Commun. Chem.*, 2019, **2**, 51.
20 R. Wang, W. Leng, Y. Gao and L. Yu, Microemulsion-like aggregation behaviour of an LCST-type ionic liquid in water, *RSC Adv.*, 2014, **4**, 14055–14062.
21 S. Ito, T. Sugiyama, N. Toitani, G. Katayama and H. Miyasaka, Application of Fluorescence Correlation Spectroscopy to the Measurement of Local Temperature in Solutions under Optical Trapping Condition, *J. Phys. Chem. B*, 2007, **111**, 2365–2371.
22 R. Karmakar and A. Samanta, Solvation Dynamics of Coumarin-153 in a Room-Temperature Ionic Liquid, *J. Phys. Chem. A*, 2002, **106**, 4447–4452.
23 J. E. Lewis and M. Maroncelli, On the (uninteresting) dependence of the absorption and emission transition moments of coumarin 153 on solvent, *Chem. Phys. Lett.*, 1998, **282**, 197–203.
24 Y.-Z. Zheng, Y. Zhou, G. Deng, R. Guo and D.-F. Chen, The structure and interaction properties of two task-specific ionic liquids and acetonitrile mixtures: A combined FTIR and DFT study, *Spectrochim. Acta, Part A*, 2020, **226**, 117641.
25 P. Verma and H. Pal, Aggregation Studies of Dipolar Coumarin-153 Dye in Polar Solvents: A Photophysical Study, *J. Phys. Chem. A*, 2014, **118**, 6950–6964.
26 Y. Kayama, T. Ichikawa and H. Ohno, Transparent and colourless room temperature ionic liquids having high refractive index over 1.60, *Chem. Commun.*, 2014, **50**, 14790–14792.